

Graphene based Ultra-Thin Flat Lenses

Xiang-Tian Kong¹, Ammar A. Khan^{2,#}, Piran R. Kidambi^{2,#}, Sunan Deng^{3,#}, Ali K. Yetisen⁴,
Bruno Dlubak², Pritesh Hiralal², Yunuen Montelongo², James Bowen⁵, Stéphane Xavier⁶,
Kyle Jiang³, Gehan A. J. Amaratunga², Stephan Hofmann², Timothy D. Wilkinson², Qing
Dai^{1,*}, Haider Butt^{3,*}

¹National Center for Nanoscience and Technology, Beijing 100190, China

²Electrical Engineering Division, Department of Engineering, University of Cambridge,
Cambridge CB3 0FA, UK

³School Mechanical Engineering, University of Birmingham, Birmingham B15 2TT, UK

⁴Harvard Medical School and Wellman Center for Photomedicine, Massachusetts General
Hospital 50 Blossom Street, Boston, MA 02114, USA

⁵School Chemical Engineering, University of Birmingham, Birmingham B15 2TT, UK

⁶Thales Research and Technology, 91767 Palaiseau, France

*Email: daiq@nanoctr.cn, Tel: +86 10 82545720.

*Email: h.butt@bham.ac.uk, Tel: +44 121 4158623

KEYWORDS Graphene, thin lenses, Fresnel zone plates

ABSTRACT: Flat lenses when compared to curved surface lenses have the advantages of being aberration free and they offer a compact design necessary for a myriad of electro-

optical applications. In this paper we present flat and ultra-thin lenses based on graphene, the world's thinnest known material. Monolayers and low number multilayers of graphene were fabricated into Fresnel zones to produce Fresnel zone plates which utilize the reflection and transmission properties of graphene for their operation. The working of the lens and their performance in the visible and terahertz regimes was analyzed computationally. Experimental measurements were also performed to characterize the lens in the visible regime and a good agreement was obtained with the simulations. The work demonstrates the principle of atom thick graphene-based lenses, with perspectives for ultra-compact integration.

Fresnel zone plates are diffractive optical elements capable of focusing light. Unlike curved lenses, Fresnel zone plates are based in diffractive rings that deform the field.(1) When the rings are properly designed it is possible to produce constructive interference at a given focal point. Binary intensity Fresnel zone plates use a flat surface with a set of radially symmetric rings, which alternate between opaque and transparent.(2) Fresnel zone plate offers the possibility of designing high numerical aperture (NA) lens with low weight and small volume. It is hence, widely used in silicon based electronics with various applications, such as optical interconnects,(3) integrated optics,(4) beam focusing(5, 6) and maskless lithography systems.(7)

In this paper we demonstrate Fresnel zone plates (FZP) based lenses made by graphene. Each graphene FZP lens has twenty four zones, with a radius of about 50 μm . This is a major achievement in realizing efficient ultrathin lenses, which has the potential to improve the capabilities of compact optical systems, such as laser focusing for optical storage and fibre-optic communication.

A thin lens is defined as one with a thickness that is negligible compared to the focal length of the lens. Currently, lenses are not thin or flat enough to remove distortions, which limit imaging. Previously aberration was corrected by techniques such as aspheric shapes or

multilens designs, resulting in heavy weight and extra space. Hence, it is very important to develop ultrathin lenses and FZPs offers a suitable solution. From the theoretical perspective a diffractive element like FZPs can achieve efficiencies close to 100% with diffraction limited performance(8, 9). However, the physical constrains limits these possibilities. For instance, the relief of the diffractive plane is one of the sources of multiple aberrations in the focal plane.(10) Therefore, thin diffraction elements are desirable for the reduction of such distortions.

The ultrathin lens based on 60 nm thick gold metasurface, fabricated by Federico Capasso *et al.*,(11) is considered to be a milestone to revolutionise consumer technology form factor. Here we report on the development of an ultrathin FZP lens using graphene on glass with a few nanometers thickness. Graphene is a single two-dimensional (2D) layer of carbon,(12) exhibiting an unique set of opto-electronic properties, in particular high optical transparency, low reflectance and a high carrier mobility at room temperature.(13, 14) This enables multiple functions of signal emitting, transmitting, modulating, and detection to be realized in one material(15) and makes graphene a promising choice for optoelectronic devices.(16) In the visible regime, the optical transmittance of single layer graphene is frequency-independent and solely determined by the fine structure constant $\alpha=e^2/\hbar c$ (c is the speed of light): $T \equiv \left(1 + \frac{2\pi G}{c}\right)^{-2} \approx 1 - \pi\alpha \approx 0.977$, in which $G = e^2/4\hbar$ is universal conductivity of graphene(17). Compared with the transmittance, the reflectance of graphene under normal light incidence is relatively weak with $R = 0.25\pi^2\alpha^2T = 1.3 \times 10^{-4}$.

However, the opacity of multi-layer graphene will increase linearly with the number of layers, N , ($T \approx 1 - N\pi\alpha$). Unlike single-layer graphene, according to Skulason *et al.*,(18) few-layer graphene could have very high reflection contrast, indicating the possibility of making FZP lens of graphene on glasses. For the FZP based lenses the focal length f of the lens is related to the radii r of successive zone edges. By means of an approximation for large

focal lengths, the radii of the rings can satisfy the equation: $\frac{f}{r_n} = \frac{r_n}{n\lambda}$ (λ is the wavelength of light, $n = 1, 2, 3\dots$), and the radius of the n th zone (r_n) in a FZP lens is given by $r_n = \sqrt{nr_1}$.(19) Setting the focal length to $\sim 120 \mu\text{m}$ at an optical wavelength of 850 nm, the spacing and widths of the Fresnel zones were calculated with different n . Figure 1 shows the three-dimensional (3D) schematic diagram of the FZP geometry and its operation. The radius of the central zones was $10 \mu\text{m}$ and the lens radius of about $49 \mu\text{m}$.

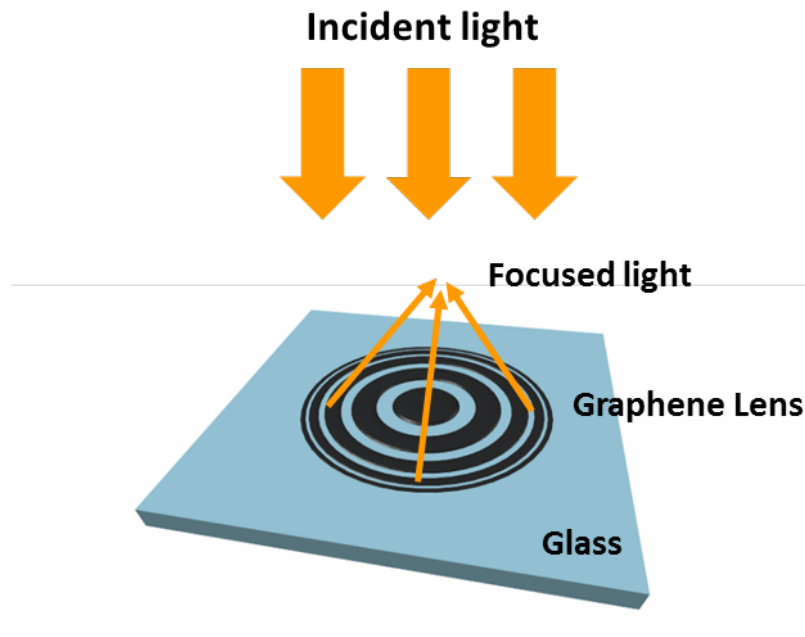


Figure 1. Schematic showing the geometry and reflection mode operation of the graphene Fresnel zone plate, incident light from the top.

The graphene FZP was simulated by the finite element method, in which the lens is illuminated perpendicularly by a plane wave. The graphene is modelled as a material with equivalent permittivity given by $\epsilon_g = i\sigma/\epsilon_0\omega t_g$,(20) where ϵ_0 is the vacuum permittivity, ω is the angular frequency of light, $t_g = 0.335 \text{ nm}$ is the monolayer graphene thickness and σ is the optical conductivity of graphene obtained from the Kubo formula.(21) In the Kubo formula, the conductivity is a function of the angular frequency ω , the Fermi level relative to the Dirac point E_F , the relaxation time τ and temperature T . The relaxation time is obtained from $\tau =$

$\mu E_F / e v_F^2$, where $\mu = 3000 \text{ cm}^2/(\text{Vs})$ is the measured dc mobility,(22) e is the electron charge and $v_F = 1 \times 10^6 \text{ m/s}$ is the Fermi velocity. The temperature is assumed to be 300 K. Note that the optical responses of graphene are not influenced by the sign of Fermi level (p -doped or n -doped), owing to the linear electron dispersion relation of graphene. The thickness of the N -layer graphene is set to be equal to Nt_g in the simulations. The optical constant of the glass substrate is obtained from a Drude model fitted from the empirical data.(23) The Drude model of silica glass is given by $\varepsilon_{\text{glass}} = \varepsilon_{\infty} - \omega_0^2 / (\omega^2 - \omega_r^2 + i\Gamma\omega)$, where $\varepsilon_{\infty} = 2.11$, $\omega_0 = 0.111 \text{ eV}$, $\omega_r = 0.132 \text{ eV}$, $\Gamma = 0.00882 \text{ eV}$. To obtain the scattered electromagnetic field (\mathbf{E}_{sc} and \mathbf{H}_{sc}), the incident field is subtracted from the computed total field. Then, the scattered power flow distribution is calculated according to the Poynting theorem, $P_{\text{sc}} = \mathbf{E}_{\text{sc}} \times \mathbf{H}_{\text{sc}}^*$.

Figure 2(a) shows the computed power flow distribution of the reflected light by the FZP made by 5-layer graphene, illuminated by light with 850-nm wavelength. The radius of the innermost graphene zone is $10 \text{ }\mu\text{m}$. Thus the theoretical focal length is $117.6 \text{ }\mu\text{m}$. The horizontal and vertical cross-sectional lines at the focal point are shown in Figures 2(b) and (c) (solid lines), respectively. Here the Fermi level is assumed to be 0.1 eV . This simulation confirms the focusing of the reflected light of the graphene-based lens. In principle, the lensing effect of FZPs is determined by the reflection contrast between a silica glass surface and the zones covered by graphene. In visible and near infrared, the reflectance of a silica surface under perpendicular illumination from air is less than 3.5%. In contrast, the reflectance of graphene-covered silica surface is much greater, see Figure 2(d). For instance, the reflectance of ten-layer graphene on silica is 6.5%, which is nearly twice of that of a bare silica surface. The reflection of Fresnel zones increases with increasing number of graphene layers. Hence, the focusing efficiency, defined as the ratio of the focal intensity to the intensity of incident light, relies mainly on the number of layers of graphene for the incident light in the visible and near infrared frequency range. For example, the dashed lines in

Figures 2(b) and (c) show the cross sectional lines corresponding to a lens composed of 10-layer graphene. As shown, the intensity of reflected light at the focal point increases two-fold when the layer number increases from 5 to 10.

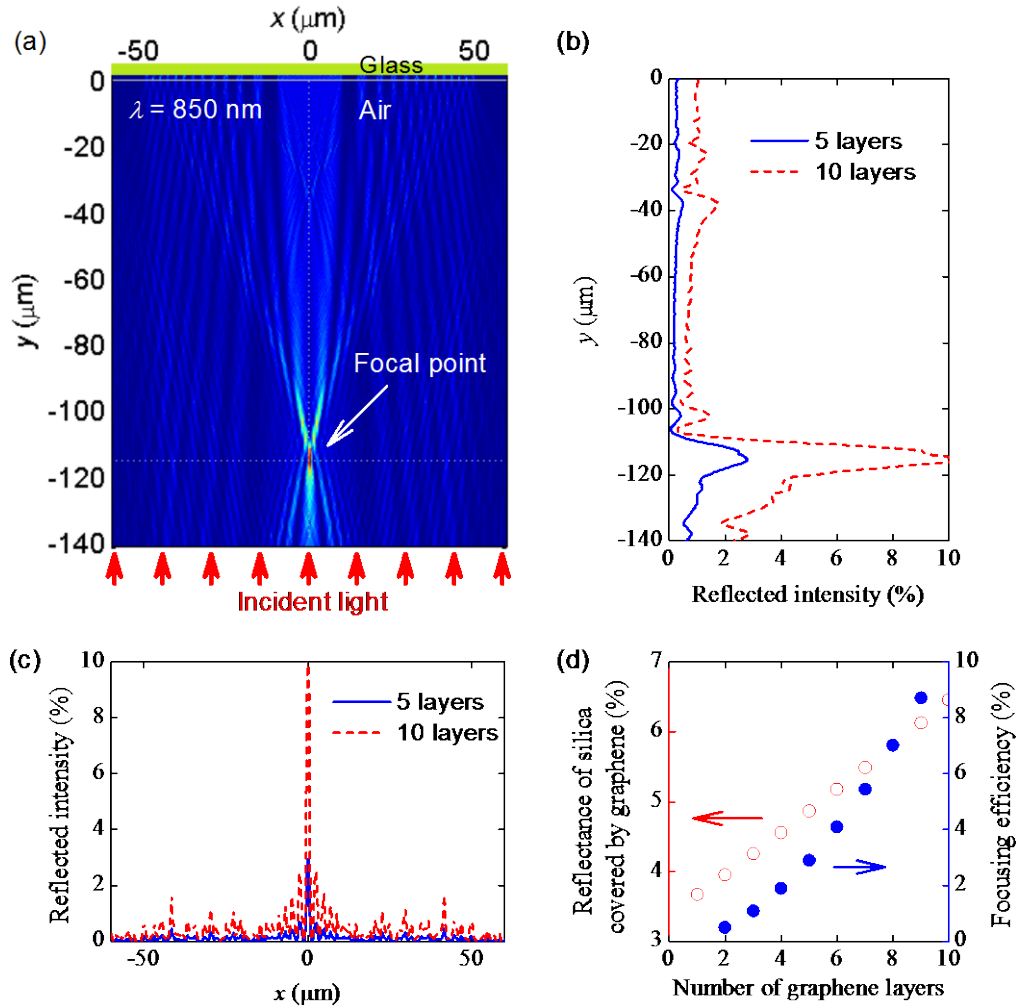


Figure 2. (a) Typical power flow distribution of the reflected light of the FZP. The lenses are located at $y = 0$ on glass substrate ($y > 0$). Light of 850-nm wavelength is illuminated from the bottom boundaries of the computation domains. (b) Light intensity in terms of y extracted at $x = 0$. (c) Light intensity in terms of x at the focal plane. In (b) and (c), solid and dashed lines correspond with lens with 5- and 10-layer graphene, respectively. (d) Reflectance of silica surface covered by graphene and focusing efficiency of FZPs with respect to the number of graphene layers. The reflectance is calculated according to Fresnel formula.

Our graphene samples grown by chemical vapour deposition were hole-doped, and their Fermi level was less than ~ 0.25 eV.(22, 24) The lens focusing effect mainly depends on the graphene's permittivity(25) so we studied both real and imaginary part of 5-layer graphene with different Fermi levels and different carrier mobility when illuminated with a 850nm light source, as shown in Figure 3(a)(b). In visible regime, the conductivity of graphene is dominated by interband, and it is nearly constant due to Pauli blocking and the Fermi level lower than the interband onset ($2|E_F| < \hbar\omega$). Table 1 presents the focusing efficiency of the 5-layer graphene lens under Fermi level ranging from 0.05 eV to 0.6 eV. This Fermi level range is less than the interband onset value (0.73 eV for incident wavelength of 850 nm), resulting in a nearly constant focusing efficiency of approximately 2.9% for the FZP made of 5-layer graphene. Table 1 presents the focusing efficiency of the 5-layer graphene lens under Fermi level ranging from 0.05 eV to 0.6 eV. This Fermi level range is less than the interband onset value (0.73 eV for incident wavelength of 850 nm), resulting in a nearly constant focusing efficiency of approximately 2.9% for the FZP made of 5-layer graphene.

Table 1. Change in the focal intensity of the lens with the Fermi level¹.

Fermi level (eV)	Focusing efficiency (%)
0.05	2.8924
0.1	2.8920
0.2	2.8894
0.3	2.8824
0.4	2.8696
0.5	2.8561
0.6	2.8860

¹ with mobility μ equal to $3000 \text{ cm}^2/(\text{Vs})$ for lens with 5-layer graphene under illumination of 850 nm wavelength

At the same time, we may notice that there are sharp peak in real permittivity and a razor edge in imaginary permittivity at the interband onset Fermi level 0.73eV. So we compared the focal intensity with carrier mobility of 10000 $\text{cm}^2/(\text{Vs})$ at Fermi level 0.1eV, 0.73eV, as well as 0.9eV, as can be seen in Figure 3 (c) and (d), which are focal intensity distribution in the vertical and horizontal cross respectively. At Fermi level 0.73eV, the focal intensity is much higher than the other two Fermi levels mainly due to higher real permittivity part, with which more light will be reflected. The lowest focal intensity at Fermi level 0.9eV is due to the lowest real permittivity.

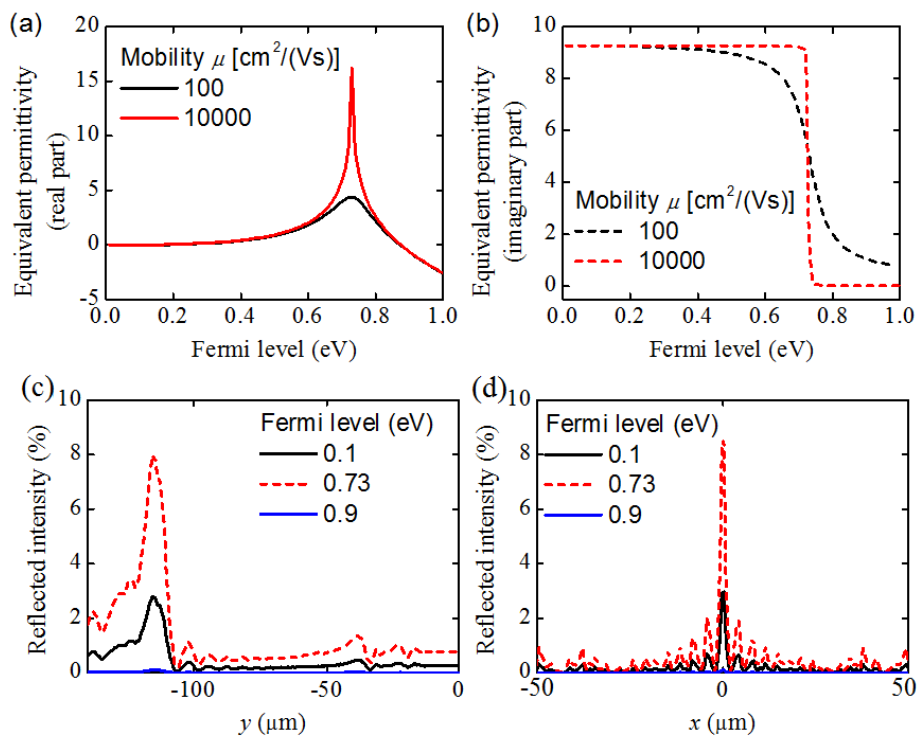


Figure 3. Properties of 5-layer graphene and graphene Fresnel lens when incident light 850nm. (a) Real and imaginary part (b) of graphene permittivity at different carrier mobility. Focal intensity distribution at different Fermi levels for graphene FZP when (c) $x=0$ and (d) y at the focal plane.

According to the Kubo formula,(21) the conductivity of graphene is a function of the relaxation time τ , which is proportional to the charge mobility. As a consequence, in general the lensing effect of FZPs varies as the charge mobility. In Figure 3(a) (b), we also studied the effect of carrier mobility on permittivity of graphene. The red line represents for

permittivity with carrier mobility $10000 \text{ cm}^2/(\text{Vs})$, while the black line with carrier mobility $100 \text{ cm}^2/(\text{Vs})$. The carrier mobility only causes a peak in the permittivity near the interband onset (0.73eV), while it shows no effect on permittivity for other values of Fermi level.

As shown in Figure 4(a), the focusing efficiency of the FZP made of 5-layer graphene increases with increasing mobility for a fix Fermi level ($E_F > 0.3 \text{ eV}$). However, the charge mobility has negligibly small influence on the focused intensity distribution of the Fresnel zone plate in a broad range of $100 \sim 10,000 \text{ cm}^2/(\text{Vs})$ when the Fermi level of graphene is small ($E_F < 0.3 \text{ eV}$). Figure 4(b) shows the focused intensity plots across the focal plane at Fermi level of 0.3 eV . With the charge mobility increasing from 100 to $10,000 \text{ cm}^2/(\text{Vs})$, no obvious change in the intensity profile can be observed. Figure 4(c) and (d) demonstrate the effect of carrier mobility on the lens focal intensity on interband onset. The mobility plays an important role at this special Fermi level, with higher carrier mobility leads to higher focal intensity.”

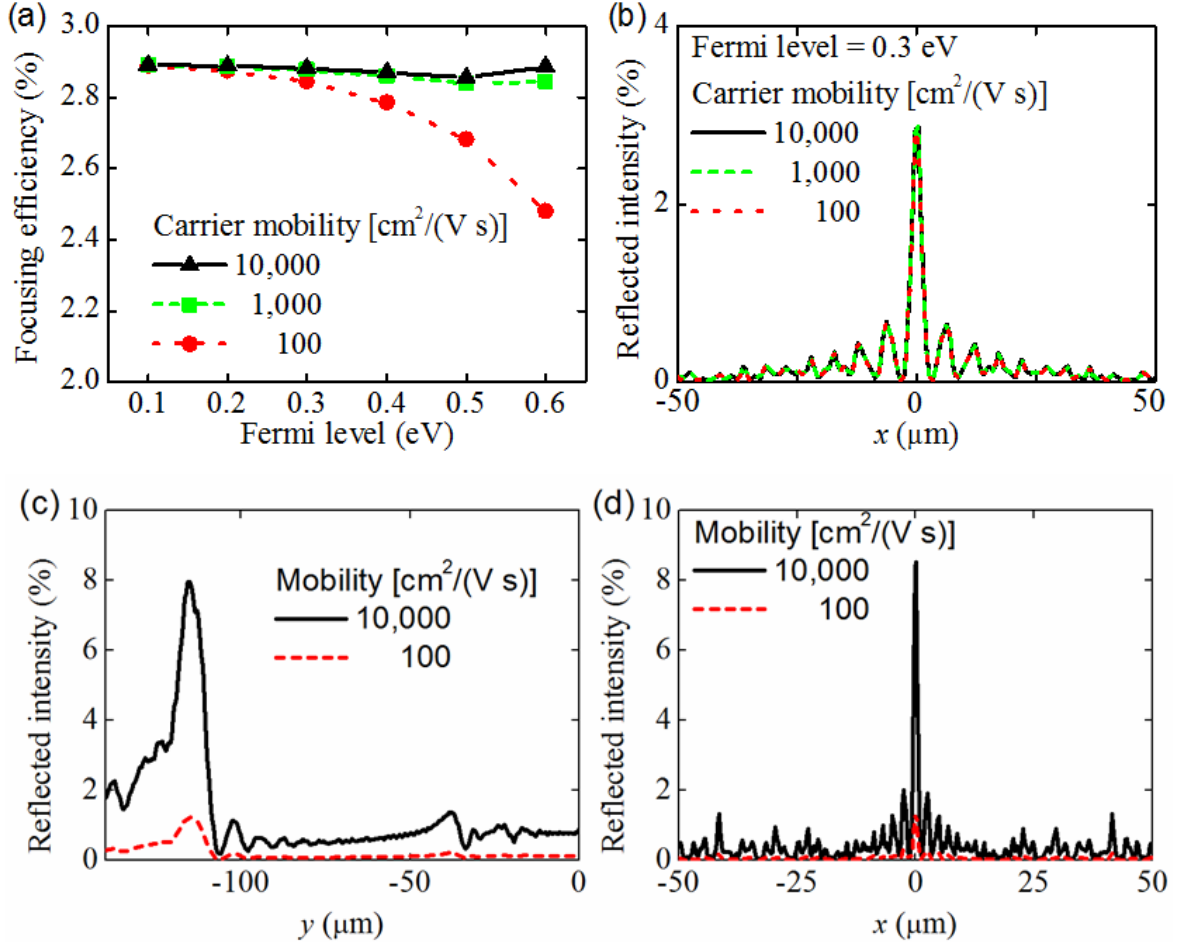


Figure 4. Effect of charge mobility on lensing effect of graphene FZPs. (a) Focusing efficiency in terms of graphene Fermi level at charge mobility of 10000, 1000, and 100 cm²/(Vs). (b) Reflected intensity at the focal plane with Fermi level of 0.3 eV and carrier mobility of 10000, 1000, 100 cm²/(Vs). (c),(d) Focal intensity distribution with different carrier mobility at interband onset 0.73eV on horizontal and vertical cross-sections respectively. Here the FZP is made of 5-layer graphene and illuminated by light of 850 nm wavelength.

Based on the simulation results mono (22, 24) and multi-layer graphene (26, 27) were synthesized by chemical vapour deposition (CVD) and Fresnel zone plates were fabricated by photolithography methods. The as-fabricated graphene lens array was characterized under an optical microscope. Figure 5(a) shows the lens array under the microscope, while Figure 5(b)

showing the lens array focusing the light with excellent contrast. Figure 5(c) and (d) demonstrate the magnified version of a single graphene FZP lens and focal point along with the light intensity profile across the horizontal direction. It was clear from the intensity profiles that the focal point exhibits a good contrast. The experimental focal length of graphene Fresnel lens is $175\mu\text{m}\pm 10\mu\text{m}$, with visible incident light. The simulations were performed for 850 nm and not the visible light due to the large amount of computational memory required. However, theoretically predicted focal length for the visible light (in the range 540.5 nm - 606nm) was $175\mu\text{m} \pm 10\mu\text{m}$. Hence, experimental data correspond well with the expected value.

The lateral width of the experimentally measured focal spot is different from the simulations due to different light sources used. In the simulations, a monochromatic light source (wavelength 850 nm) was used to demonstrate the lensing effect of clearly. Whereas in the experiments, a broad band white light source was used. Thus the measured focus spot had a much wider area as it is a net combination of many focus points made by different wavelengths.

The focusing efficiency of the lens is 6.57%, which is calculated from the ratio of light intensity at the focal point to the incident light intensity falling on lenslet. The experimental focal efficiency corresponds well with the calculated value 6.6% for 9-layer graphene, shown in Figure 2(d) (given that the graphene reflectance is constant across the visible range and 850 nm). The maximum efficiency reported for the ultrathin lens based on 60 nm thick gold metasurface is approximately 1% for wavelength of 1550 nm.(11) Also designing such metasurface lenses for the visible range will be a challenge due to the fine nanoscaled structures required. The graphene based lenses offer more compactness, lower losses, are much easier to fabricate and also offer tunability in the infra-red range.

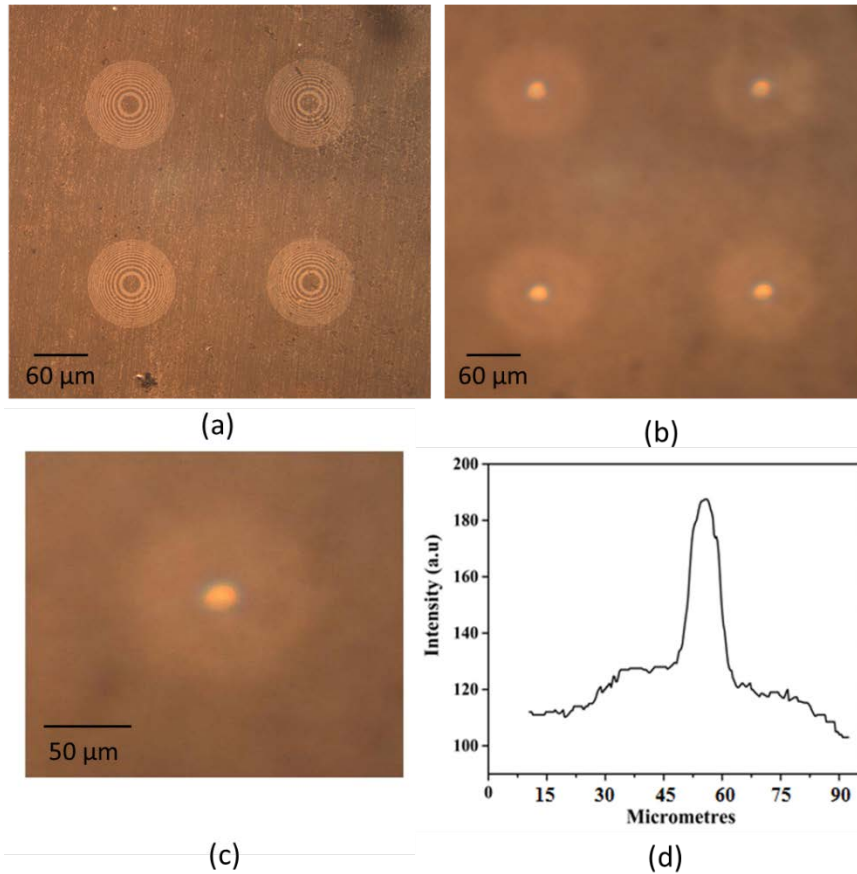


Figure 5. Graphene FZP lens array under a reflection mode dark field optical microscopy: (a) optical image of the graphene FZP lens array. Each lenslet has twenty four zones and the radius of the centre zone is 10μm. (b) Graphene FZP showing the light focusing with excellent contrast. (c) Single FZP focusing spot. (d) Light intensity across the horizontal axis of the focal point in (c).

The lens arrays produced worked both in reflection and transmission mode of operation. In the transmission mode the focal point was produced within the glass substrate. Figure 6 shows the magnified version of a single graphene lens and focal points for two modes of operation. In figure 6(a), the dark zones are glass and the bright zones are graphene, which shows the good reflection optical contrast of few layer graphene on glass. By adjusting the focusing position of microscopy, we could get focusing spots both in glass (as show in figure 6(b), transmission mode) and in air (as show in figure 6(c), reflection mode).

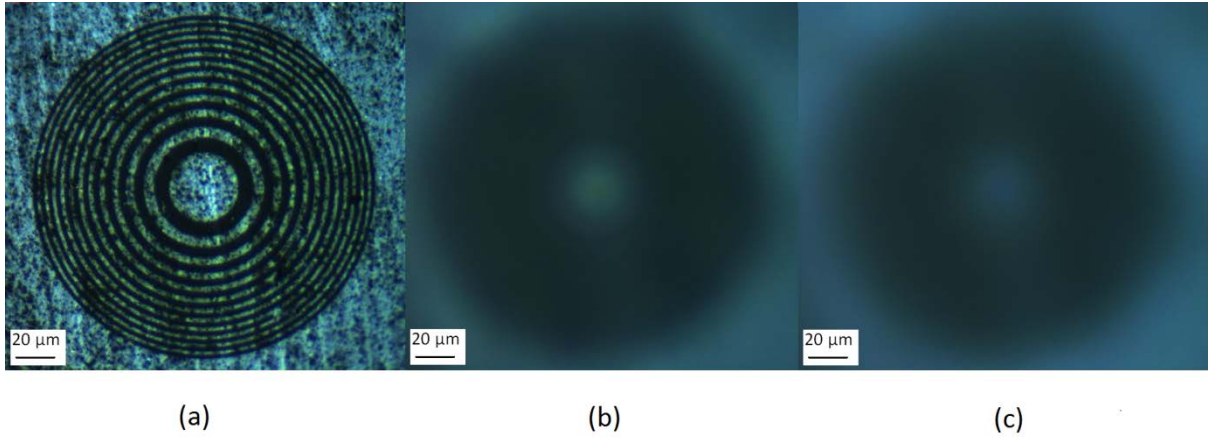


Figure 6. A single graphene FZP lenslet zoomed under optical microscope. (a) Magnified single graphene lenslet. (b) Graphene lens work as a transmission lens. (c) Graphene lens work as a reflection lens

To study the surface profile of the multi-layered graphene lens, studies were carried out in atomic force microscope (AFM). AFM image of a single graphene FZP is shown in figure 7. The bright spots in Figure 7(a) arise from the polymer residue post lithography and lead to artifacts in AFM images i.e. the black lines in Figure 7(a). Figure 7(b) shows the information of the height distribution along the blue line. The Fresnel zones were clearly visible in the surface profile and the average surface roughness was measured as 3.47nm, which corresponds to approximately 10 layers of graphene. A few peaks in the range of 8-10 nm range are observed due to the left over polymer residues.

Optical transmission measurements were also performed for the multilayer graphene which was used for making the FZPs. An ocean optic spectrometer connected to the optical microscope was used to measure the transmission spectra. Transmission spectra for glass and graphene on glass were measured as shown in Figure 7(c). The results show that compared to the bare glass substrate, graphene sample transmitted about 75-78% of the incident light. Theoretically, the transmission of 10 layer graphene is given by: $T \approx 1 - N\pi\alpha \approx 77\%$. So the measured data is in good agreement with the theoretical calculation.

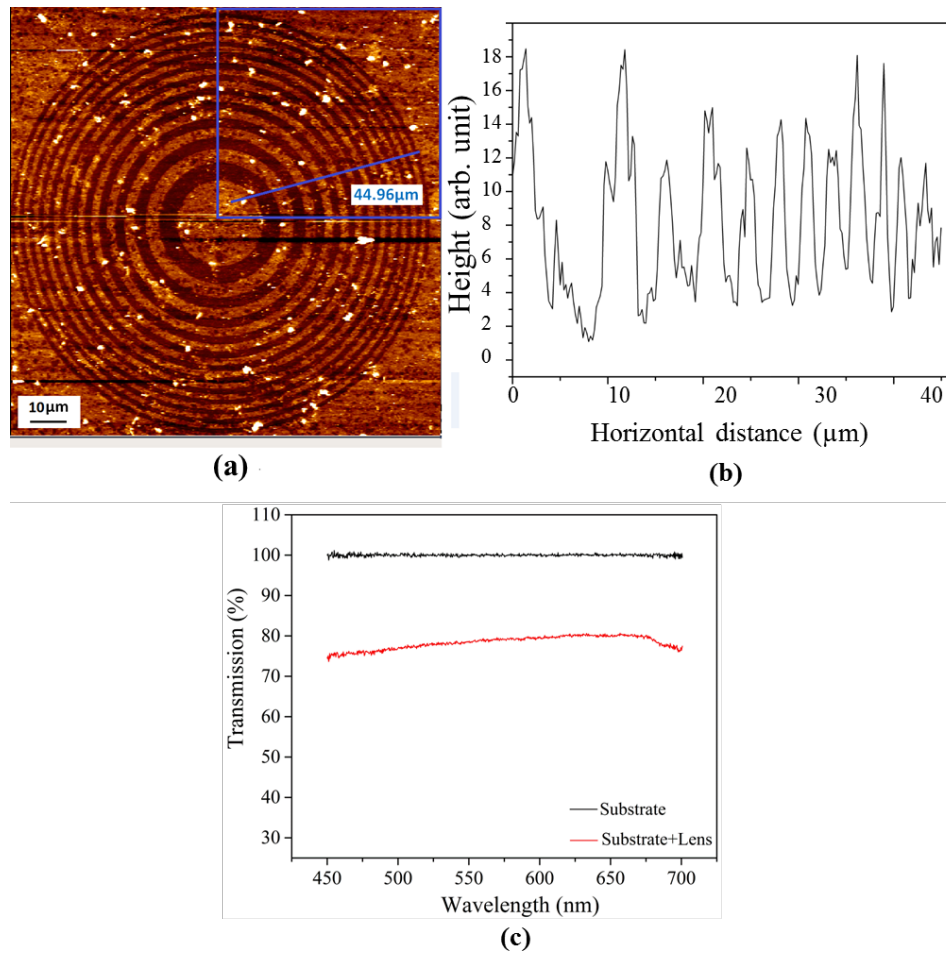


Figure 7. (a) AFM image of single graphene FZP. (b) Roughness distribution along the blue line. (c) Transmission spectrum for multi-layered graphene used for producing the lens array.

Finally to demonstrate the thinnest possible lens a single layer of graphene was used. Samples consisting of monolayer graphene were patterned lithographically onto 0.7 mm thick glass using a Microtech Laser writer (LW405, minimum resolution 0.7 μm) with a 405 nm laser. A positive resist (AZ5214) was used as an etch mask, spin coated at 4000 rpm and dried at 100°C for 1 minute, resulting in a 1 μm thick resist film which was subsequently patterned with the laser and developed. The sample was then ashed under oxygen plasma (100 W, 5-10 minutes) to etch the exposed graphene layers, and subsequently washed thoroughly in acetone and 2-propanol to remove the remaining masking resist, leaving the patterned graphene surface. Figure 8(a) shows the single layered graphene FZP lens under

optical microscope; while Figures 8(e) and (g) demonstrate the same producing a focal point in the transmission and reflection modes of operation, respectively. The intensity profiles were also calculated across the focal points which demonstrate good contrast.

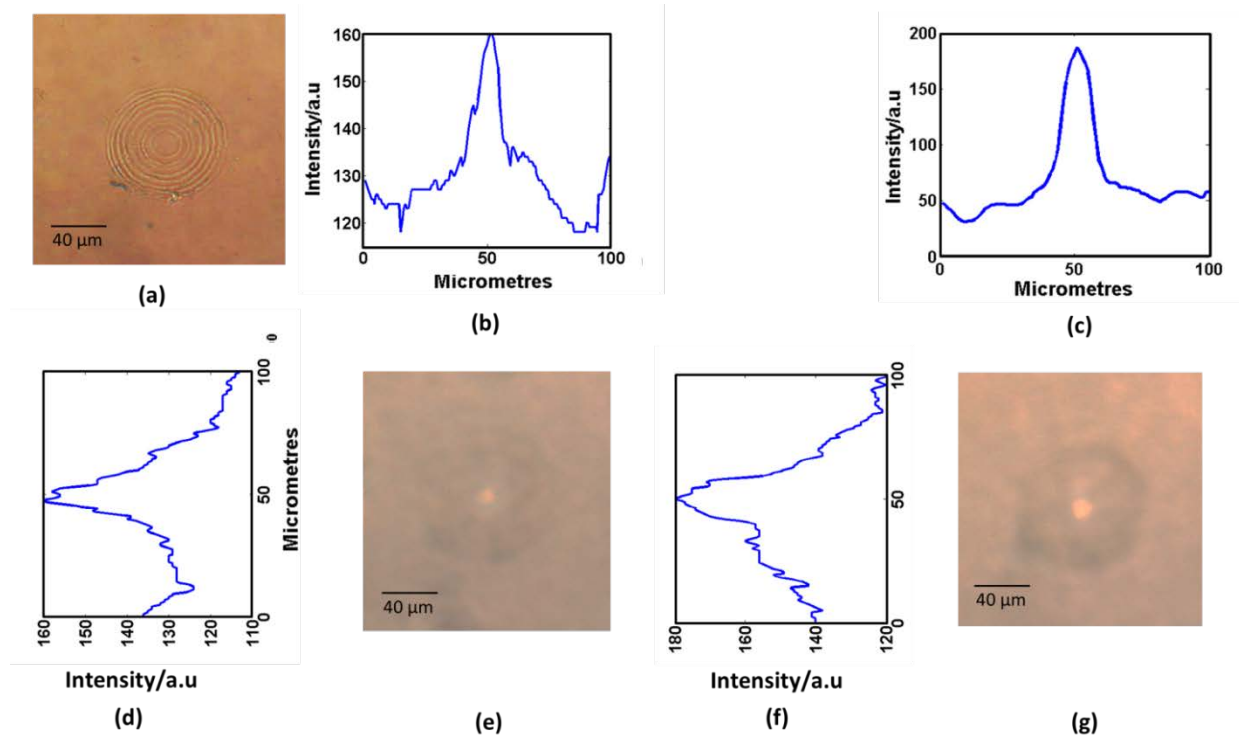


Figure 8. (a) Single layer graphene Fresnel zone plate zoomed under optical microscope. (e) and (g) show the lens working under transmission mode and reflection mode, respectively. (b) and (c) show the light intensity plots across the horizontal axis of transmission mode and reflection mode. (d) and (f) show the light intensity plots across the vertical axis of transmission mode and reflection mode focal point.

Producing the thinnest possible flat lens using the novel graphene material is a next step towards achieving high resolution, low noise and compact lenses for imaging applications. By increasing the widths of graphene based lens very high numerical apertures can also be achieved. Graphene is also being proposed as a transparent electrode for solar cells. By patterning it into the Fresnel zone plates-like geometries we demonstrated it can be simultaneously used as optical concentrator. Moreover, as a future work graphene-based flat and compact lenses will be very useful in the terahertz range. In the terahertz frequency

range, the conductivity (absorption) of graphene changes significantly with the Fermi level.(14, 28) Hence, by controlling the Fermi levels (electronically) the performance of graphene based lenses could be tuned.

In conclusion, we have developed ultrathin multi- and single-layer graphene-based Fresnel zone plate lenses on glass with nanoscale roughness. Through calculation and finite element modelling, the lenses were designed to operate in the optical regime. The lenses were fabricated by a lithography technique, and their focusing properties were characterized. The lenses were found to be thinner, more efficient, and easier to fabricate compared to the metasurface based flat lenses. Hence the graphene lens arrays are highly promising as flat and ultrathin lenses as they have the potential to revolutionize the design of compact optical systems, such as laser focusing for optical storage and fibre-optic communication.

Corresponding Author

[*h.butt@bham.ac.uk](mailto:h.butt@bham.ac.uk), Tel: +44 121 4158623, Fax: +44 121 414 3958

Present Addresses

†School of Mechanical Engineering, University of Birmingham, Edgbaston, Birmingham B15 2TT, UK

Author Contributions

The manuscript was written through contributions of all authors. All authors have given approval to the final version of the manuscript. #These authors contributed equally.

Acknowledgements

HB would like to thank The Leverhulme Trust for the research funding. QD is supported by Bureau of International Cooperation, Chinese Academy of Sciences (121D11KYSB20130013).

References

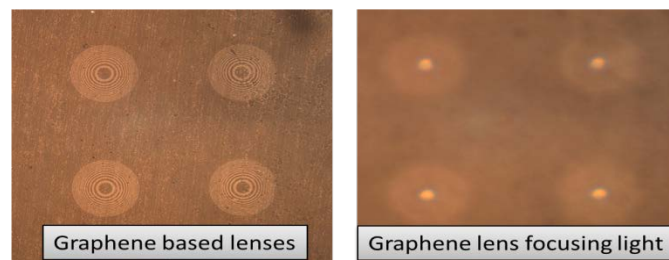
1. Aničin, B.; Babović, V.; Davidović, D. Fresnel lenses. *Am.J.Phys* 1989, 57, 312.
2. Rastani, K.; Marrakchi, A.; Habiby, S. F.; Hubbard, W. M.; Gilchrist, H.; Nahory, R. E. Binary phase Fresnel lenses for generation of two-dimensional beam arrays. *Appl.Optics* 1991, 30, 1347-1354.
3. Ferstl, M.; Frisch, A.-M. Static and dynamic Fresnel zone lenses for optical interconnections. *J.Mod.Opt* 1996, 43, 1451-1462.
4. Kodate, K.; Tokunaga, E.; Tatuno, Y.; Chen, J.; Kamiya, T. Efficient zone plate array accessor for optoelectronic integrated circuits: design and fabrication. *Appl.Optics* 1990, 29, 5115-5119.
5. Fallahi, M.; Kasunic, K. J.; Penner, S.; Nordman, O.; Peyghambarian, N. Design and fabrication of circular grating coupled distributed Bragg reflector lasers. *Opt .Eng* 1998, 37, 1169-1174.
6. Morgan, B.; Waits, C. M.; Krizmanic, J.; Ghodssi, R. Development of a deep silicon phase Fresnel lens using Gray-scale lithography and deep reactive ion etching. *J.Microelectromech.S* 2004, 13, 113-120.
7. Carter, D. J. D.; Gil, D.; Menon, R.; Mondol, M. K.; Smith, H. I.; Anderson, E. H. Maskless, parallel patterning with zone-plate array lithography. *J.Vac.Sci.Technol.B* 1999, 17, 3449-3452.
8. Perry, M.; Shannon, C.; Shults, E.; Boyd, R.; Britten, J.; Decker, D.; Shore, B. High-efficiency multilayer dielectric diffraction gratings. *Opt.Lett* 1995, 20, 940-942.
9. Menon, R.; Gil, D.; Smith, H. I. Experimental characterization of focusing by high-numerical-aperture zone plates. *JOSA A* 2006, 23, 567-571.
10. Hessler, T.; Rossi, M.; Kunz, R. E.; Gale, M. T. Analysis and optimization of fabrication of continuous-relief diffractive optical elements. *Appl.Optics* 1998, 37, 4069-4079.
11. Aieta, F.; Genevet, P.; Kats, M. A.; Yu, N.; Blanchard, R.; Gaburro, Z.; Capasso, F. Aberration-free ultrathin flat lenses and axicons at telecom wavelengths based on plasmonic metasurfaces. *Nano Lett.* 2012, 12, 4932-4936.
12. Geim, A. K.; Novoselov, K. S. The rise of graphene. *Nat. Mater.* 2007, 6, 183-191.
13. Butt, H.; Kidambi, P. R.; Dlubak, B.; Montelongo, Y.; Palani, A.; Amaratunga, G. A.; Hofmann, S.; Wilkinson, T. D. Visible Diffraction from Graphene and Its Application in Holograms. *Adv.Opt.Mater* 2013, 1, 869-874.
14. Degl'Innocenti, R.; Jessop, D. S.; Shah, Y. D.; Sibik, J.; Zeitler, J. A.; Kidambi, P. R.; Hofmann, S.; Beere, H. E.; Ritchie, D. A. Low-Bias Terahertz Amplitude Modulator Based on Split-Ring Resonators and Graphene. *ACS nano* 2014, 8, 2548-2554.
15. Bao, Q.; Loh, K. P. Graphene photonics, plasmonics, and broadband optoelectronic devices. *ACS nano* 2012, 6, 3677-3694.
16. Cooper, D. R.; D'Anjou, B.; Ghattamaneni, N.; Harack, B.; Hilke, M.; Horth, A.; Majlis, N.; Massicotte, M.; Vandsburger, L.; Whiteway, E. Experimental review of graphene. *Condens.Mat.Phys* 2012, 2012.

17. Nair, R.; Blake, P.; Grigorenko, A.; Novoselov, K.; Booth, T.; Stauber, T.; Peres, N.; Geim, A. Fine structure constant defines visual transparency of graphene. *Science* 2008, 320, 1308-1308.
18. Skulason, H.; Gaskell, P.; Szkopek, T. Optical reflection and transmission properties of exfoliated graphite from a graphene monolayer to several hundred graphene layers. *Nanotechnology* 2010, 21, 295709.
19. Fan, Y.-H.; Ren, H.; Wu, S.-T. Switchable Fresnel lens using polymer-stabilized liquid crystals. *Opt. Express* 2003, 11, 3080-3086.
20. Vakil, A.; Engheta, N. Transformation optics using graphene. *Science* 2011, 332, 1291-1294.
21. Gusynin, V.; Sharapov, S.; Carbotte, J. Magneto-optical conductivity in graphene. *J.Phys-Condens.Mat* 2007, 19, 026222.
22. Kidambi, P. R.; Ducati, C.; Dlubak, B.; Gardiner, D.; Weatherup, R. S.; Martin, M.-B.; Seneor, P.; Coles, H.; Hofmann, S. The parameter space of graphene chemical vapor deposition on polycrystalline Cu. *J. Phys.Chem C* 2012, 116, 22492-22501.
23. Palik, E. D. Handbook of Optical Constants of Solids: Index. Access Online via Elsevier: 1998.
24. Kidambi, P. R.; Bayer, B. C.; Blume, R.; Wang, Z.-J.; Baehtz, C.; Weatherup, R. S.; Willinger, M.-G.; Schloegl, R.; Hofmann, S. Observing graphene grow: catalyst–graphene interactions during scalable graphene growth on polycrystalline copper. *Nano Lett.* 2013, 13, 4769-4778.
25. Deng, S.; Yetisen, A. K.; Jiang, K.; Butt, H. Computational modelling of a graphene Fresnel lens on different substrates. *RSC.Adv.* 2014, 4, 30050-30058.
26. Kidambi, P. R.; Bayer, B. C.; Weatherup, R. S.; Ochs, R.; Ducati, C.; Szabó, D. V.; Hofmann, S. Hafnia nanoparticles—a model system for graphene growth on a dielectric. *Physica status solidi (RRL)* 2011, 5, 341-343.
27. Xi, K.; Kidambi, P. R.; Chen, R.; Gao, C.; Peng, X.; Ducati, C.; Hofmann, S.; Kumar, R. V. Binder free three-dimensional sulphur/few-layer graphene foam cathode with enhanced high-rate capability for rechargeable lithium sulphur batteries. *Nanoscale* 2014, 6, 5746-5753.
28. Badhwar, S.; Sibik, J.; Kidambi, P. R.; Beere, H. E.; Zeitler, J. A.; Hofmann, S.; Ritchie, D. A. Intrinsic terahertz plasmon signatures in chemical vapour deposited graphene. *Appl.Phys.Lett* 2013, 103, 121110.

For Table of Contents Use Only

Graphene based Ultra-Thin Flat Lenses

Xiang-Tian Kong¹, Ammar A. Khan^{2,#}, Piran R. Kidambi^{2,#}, Sunan Deng^{3,#}, Ali K. Yetisen⁴,
Bruno Dlubak⁵, Pritesh Hiralal², Yunuen Montelongo², James Bowen⁶, Stéphane Xavier⁵,
Kyle Jiang³, Gehan A. J. Amaratunga², Stephan Hofmann², Timothy D. Wilkinson², Qing
Dai^{1,*}, Haider Butt^{3,*}



Size: 1.375 inches high x 3.5 inches wide

Brief synopsis:

We have designed an ultrathin flat lens based on few layers graphene. Using conventional nanofabrication techniques, we patterned the samples of graphene into circular zones known as Fresnel zones. When light passed through these zones, it diffracts and is focused in the focal plane. The performance of these lenses has been characterized both theoretically and experimentally, and good agreement is achieved between the both. The figure below shows graphene based lenses performing focusing of light.